Q. J. R. Meteorol. Soc. (1995), **121**, pp. 783–796

CISK: A theory for the response of tropical convective complexes to variations in sea surface temperature

By JOHN L. McBRIDE[1] and KLAUS FRAEDRICH[2]*

[1]*Bureau of Meteorology Research Centre, Australia*
[2]*Meteorologisches Institut der Universität Hamburg, Germany*

(Received 25 May 1994; revised 21 October 1994)

SUMMARY

A set of balanced and unbalanced slab-symmetric linear 2-layer models is analysed. The stability properties depend on a parametrized moisture budget dominated by the value of the underlying sea surface temperature. Convective heating occurs within an inner region characterizing the size of the convective disturbance. The heating is equal to the sum of two terms, representing the mid-level and lower-level upward mass-fluxes.

A fast and a slow mode of instability can be distinguished. The slow mode shows finite maximum growth for infinitesimally small disturbances and is the instability traditionally associated with Conditional Instability of the Second Kind (CISK). The fast mode reveals infinitely large positive growth-rates for finite-size disturbances.

The transition of the model solution from slow to fast mode occurs at a threshold value of sea surface temperature. For the parameters chosen in this study, the threshold occurs at approximately 25.5 °C.

KEYWORDS: CISK Convective complexes Cumulus parametrization Sea surface temperature Tropical convection

1. INTRODUCTION

Several authors have documented the way in which, over the tropical oceans, the organization of cumulonimbus activity into weather systems depends in a highly non-linear manner on the value of the underlying sea surface temperature (SST) (e.g. Palmèn 1948; Gray 1968; Lau and Chan 1988; Merrill 1988; Webster and Lukas 1992; Evans 1993). In this paper we show that a dynamical mechanism reproducing this behaviour is contained in the two-layer model of Charney and Eliassen (1964) (hereafter referred to as CE64). CE64 was a landmark paper in the field, as it was one of two papers proposing the theory of CISK, or Conditional Instability of the Second Kind, the other being that of Ooyama (1964).

The diagram of growth rate σ (vertical axis) versus horizontal scale L (horizontal axis), reproduced from CE64 is shown in Fig. 1(a). To present our argument, we discuss two aspects of this figure. The first relates to the family of curves in (σ, L) space. Each curve is designated by a value of the parameter μ which in the cumulus parametrization proposed by CE64 represented a mean tropospheric value of relative humidity. In the formulation of CE64, the vertically integrated total heating in a column is proportional to the vertically integrated moisture-convergence (including the 'evaporative' flux from the lower boundary); and the key parameter governing variations in this is the relative humidity μ. The fundamental hypothesis of the present paper is that the variations in integrated moisture-convergence are governed not by an *internal* parameter such as the relative humidity; but rather by an *external* parameter such as the SST or its proxy the low-level saturation specific humidity.

This leads to our representation of the growth-rate curves as shown in Fig. 1(b). It should be immediately noted that this representation gives a very rapid change in the character of the solution at temperatures around 25 to 26 °C .

The second aspect to note in Fig. 1(a) is that there are two distinct instabilities present. The curves labelled with $\mu = 0.7$, 0.8, 0.9 represent what we shall refer to in this paper as the 'slow mode' whereas that labelled $\mu = 1.0$ will be referred to as the 'fast mode'. The existence of these two modes has been noted by Bates (1973); but it was Mak (1981) who

* Corresponding author: Meteorologisches Institut der Universität Hamburg, Bundestrasse 55, 20146 Hamburg, Germany.

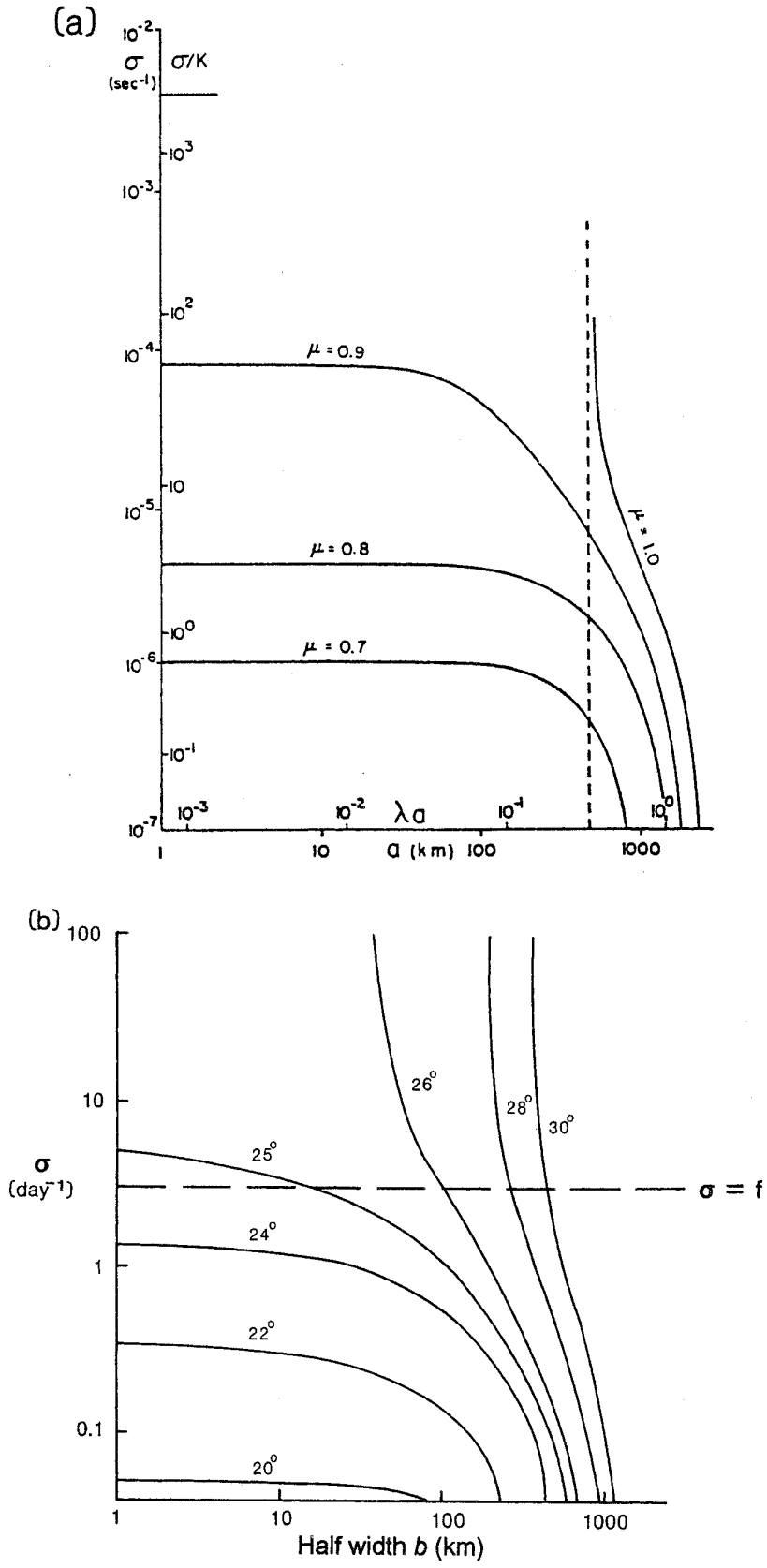

Figure 1. (a) The growth rate σ of a tropical depression as a function of the radius a of the cloud region (from Charney and Eliassen (1964) and using their notation). (b) The growth rate σ of a slab-symmetric tropical disturbance as a function of the half-width b of the convective area depending on the sea surface temperature (°C). f is the Coriolis parameter.

identified the slow mode as being associated with the component of heating proportional to the low-level vorticity, while the fast mode is forced by the component of heating directly proportional to the divergent component of the wind. The slow mode is the traditional linear CISK studied by Ooyama (1964, 1969), Charney (1973), Fraedrich and McBride (1989) and others. The fast mode, however, was dismissed by CE64 as being associated with unrealistically large values of the relative humidity μ. It was also dismissed by Mak (1981) as being unphysical, essentially because the growth rate became infinite at finite radius (marked by a vertical dashed line in Fig. 1(a)).

Fraedrich and McBride (1995) re-examined the fast-mode instability and found that in the presence of an Ekman boundary condition it gave balanced solutions at scales larger than the deformation radius. They also found that in practice the growth rate remained finite depending on the vertical structure of the initial disturbance. They compared growth rates, horizontal length scales and associated vertical mass-flux profiles against observations and concluded that the fast-mode instability may be a viable mechanism for tropical cyclone or tropical cloud-cluster development in nature. They termed the fast-mode instability 'large scale convective overturning'. Thus the second hypothesis of the present paper is that the fast mode is a physically realistic solution and is the instability responsible for the initial growth of oceanic cloud clusters and tropical cyclones in the atmosphere.

In the following section (2) we present the set of model equations, and their solutions, for the relationship between growth rate and horizontal scale. We discuss the structure and behaviour of the fast-mode solution. A moisture budget is formulated for the model, which leads to the derivation of the two versions of the cumulus parametrization: the relative-humidity-based version of CE64 and the SST-based version central to the thesis of this paper. Section 3 presents the results in terms of the dependence on SST. It shows the existence of a threshold temperature at which the solutions change from the slow domain to the fast domain, as depicted in Fig. 3. The final section (4) summarizes and attempts briefly to assess the feasibility of this mechanism for tropical cyclone and/or cloud-cluster development.

2. Model equations and solutions

CE64 employed a two-layer model in pressure coordinates for inviscid balanced perturbations about a stratified basic state at rest on an f-plane. The vertical model geometry for the dynamical equations is shown on the left-hand portion of Fig. 2. CE64 employed a cylindrical geometry with axisymmetry; but (following Charney 1973; Mak 1981; Fraedrich and McBride 1989) we can choose a slab-symmetric system such that $\partial/\partial x = 0$, without loss of generality. Following Fraedrich and McBride (1989), the model equations are the following

$$
\left.
\begin{aligned}
\sigma u_1 &= f v_1 & \sigma u_3 &= f v_3 \\
\lambda_1 \sigma v_1 + f u_1 &= -\frac{\partial \phi_1}{\partial y} & \lambda_1 \sigma v_3 + f u_3 &= -\frac{\partial \phi_3}{\partial y} \\
-\frac{p}{R_d \Delta p}\sigma(\phi_3 - \phi_1) &= \frac{S_p}{R_d}\omega_2 + \frac{Q_2}{c_p} & & \\
\frac{\partial v_1}{\partial y} + \frac{\omega_2}{\Delta p} - \frac{\omega_0}{\Delta p} &= 0 & \frac{\partial v_3}{\partial y} + \frac{\omega_4}{\Delta p} - \frac{\omega_2}{\Delta p} &= 0 \\
\omega_0 &= 0 & \omega_4 &= \lambda_2 K \frac{\partial u_3}{\partial y} \\
Q_2 &= -\frac{c_p p}{R_d} S(\eta\omega_4 + \gamma\omega_2) & |y| &< b \\
Q_2 &= 0 & |y| &> b
\end{aligned}
\right\} \qquad (1)
$$

where the dependent variables u, v, ω are the wind components in the x, y, and p directions; ϕ is (perturbation) geopotential; Q is the heating of the large scale due to cumulonimbus activity; and the subscripts 0 to 4 denote the model level at which the variable is defined. Figure 2 shows the classical two-layer model with the five levels at which the dynamic variables are defined; the related moisture variables are discussed in section 2(d). Time dependence of the solutions has been assumed to be proportional to $\exp(\sigma t)$ so that all time derivatives appear as the pre-multiplier σ, equal to the growth rate.

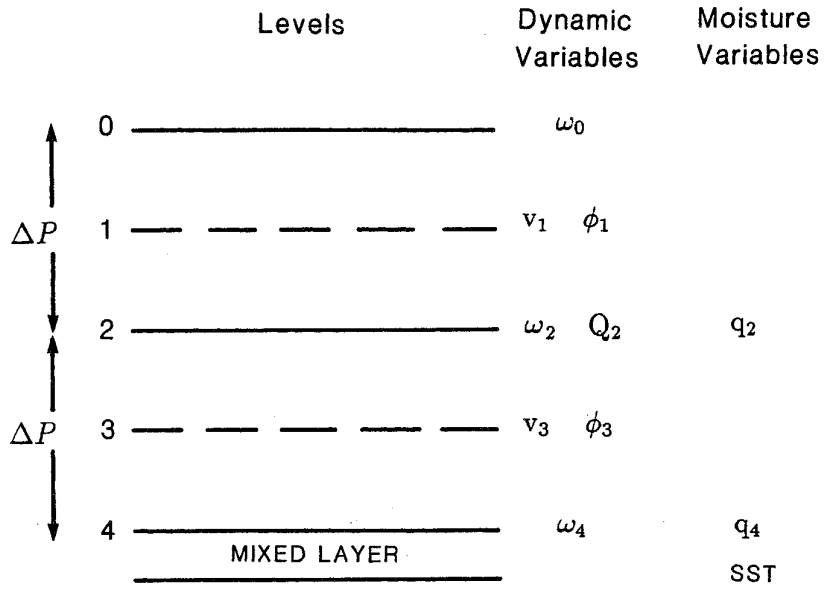

Figure 2. The two-layer model geometry of the classical Charney and Eliassen (1964) and Mak (1981) model. For notation see text.

The trace indicator λ_1 has the value zero when the quasi-geostrophic balance condition is assumed, and the value one otherwise. The trace indicator λ_2 is zero when zero mass-flux is assumed at the lower boundary, and equals one when the Ekman condition is assumed at the lower boundary. The couplet (y, p) comprises the independent variables; Δp is the half-depth of the model atmosphere (Fig. 2), f is the Coriolis parameter, R_d is the (dry) gas constant; c_p is specific heat; K is the half-depth of the boundary layer assumed to underlie the model and S is static stability.

The parameter η is a dimensionless coefficient appearing in the heating term proportional to the Ekman vertical-velocity at the lower boundary (level 4). γ is the coefficient in the heating term proportional to the total vertical velocity at level 2, the level at which the heating is applied. Thus, mathematically, $S(1-\gamma)$ is a modified static stability in the region $|y| < b$ in which the heating is applied. As will be shown below, its value is determined by the moisture budget. Following Fraedrich and McBride (1995), it may be physically interpreted as the ratio of the diabatic heating associated with the divergent part of the wind field to the adiabatic cooling.

Following standard techniques (e.g. Lilly 1960; chapter 13 of Charney 1973; Fraedrich and McBride 1989), Eqs. (1) are solved by reducing it to an ordinary differential equation in one variable in each of the domains $|y| < b$ and $|y| > b$. The horizontal boundary conditions are that all perturbation variables go to zero at $y = \infty$ and that the solutions assume a sine or cosine structure in the inner domain and an exponentially decaying form at $|y| > b$.

The demand for continuity for the normal velocities v_1, v_3 and of the geopotentials

ϕ_1, ϕ_3 at $y = \pm b$ results in a matching condition, as embodied in the following equation

$$b/R = \sqrt{\frac{\eta + (\gamma - 1)(\sigma^* + 1)}{2\sigma^* + 1}} \arctan \sqrt{\frac{\eta + (\gamma - 1)(\sigma^* + 1)}{\sigma^* + 1}}. \tag{2}$$

Once the external heating coefficients η, γ are specified, Eq. (2) is a relationship between the half-width b of the disturbance and the growth rate σ, where b has been non-dimensionalized by dividing by the Rossby deformation-radius for the problem, $R = \Delta p\sqrt{S}/f$, and the growth rate has been non-dimensionalized through the relationship

$$\sigma^* \equiv \frac{\Delta p}{Kf}\sigma \equiv \frac{\sigma}{\sigma_{\text{EKMAN}}}. \tag{3}$$

(*a*) *The width–growth relation*

Equation (2) characterizes the balanced-flow instability associated with an Ekman boundary-layer and cumulus heating and is derived by solving Eqs. (1) for $\lambda_1 = 0, \lambda_2 = 1$. This instability has been discussed by Charney and Eliassen (1964), Bates (1973), Mak (1981) and others. Other types of solutions, which are associated with a spectrum of flows, are easily derived. They are presented in Table 1 together with comments on the underlying physics and structural behaviour. The following points are noted:

The fast-mode instability is defined here as the mode associated with infinite growth-rate. Mak (1981) demonstrated that this arises through the presence of the mid-level heating coefficient γ in the thermodynamic equation of Eqs. (1). The modes described in rows 1 to 5 of Table 1 are those with this heating term present; it is seen that the infinite growth-rate arises if, and only if, γ exceeds the value *one*.

A slow-mode instability is defined as the mode associated with a finite maximum value of the growth rate σ^*. This slow (or classical CISK) mode arises in connection with the coefficient η, representing the component of heating proportional to the vertical velocity at the top of the boundary layer in Eqs. (1). Rows 1, 2, 6 and 7 of Table 1 have this heating term present. It is seen that finite growth arises if, and only if, the set of conditions ($\eta > 0$, $0 \leqslant \gamma < 1$, $\eta + \gamma > 1$) is satisfied.

In rows 1 and 2 of Table 1, the Ekman heating-term (positive η) is simultaneously present with the fast mode. For these configurations, under conditions where the fast mode is stable (i.e. $\gamma < 1$), the maximum growth-rate corresponds to $\sigma^* = (\eta + \gamma - 1)/(1 - \gamma)$. As previously noted, this is the slow-mode, or classical CISK, solution. The maximum growth-rate occurs at $b_{\text{MIN}}/R = 0$, and this intercept is the free-ride solution studied by Fraedrich and McBride (1989), Pedersen (1991) and Wiin-Nielsen (1993). For $\gamma > 1$ the growth rates increase from $\sigma = 0$ to $\sigma \to \infty$, characterizing fast modes of the model. For the balanced version of the equations (row 1), infinitely large growth-rates, $\sigma_{\text{MAX}} = \infty$, are related to finite-size perturbations, b_{MIN}/R, whose magnitude depends only on the value of γ (that is, on the mid-level mass-flux in the heating term) through the relation $b_{\text{MIN}}/R = \sqrt{(\gamma - 1)/2} \arctan \sqrt{\gamma - 1}$.

The models represented in rows 3 to 5 have only the fast mode present (i.e. η, the heating coefficient proportional to Ekman pumping, $= 0$). Unstable solutions exist for $\gamma > 1$ only and maximum (infinite) growth-rate occurs at vanishing radius for

TABLE 1. INSTABILITY PROPERTIES AND MODEL CHARACTERISTICS

Row (1)	Model (2)	Matching condition $b/R =$ (3)	Max. growth σ^* (4)	Scale b/R of max. growth b_{MIN}/R (5)	Scale b/R of zero growth b_{MAX}/R (6)
1	Fast mode and CISK mode	$\sqrt{\frac{\eta+(\gamma-1)(\sigma^*+1)}{(2\sigma^*+1)}}\arctan\sqrt{\frac{\eta+(\gamma-1)(\sigma^*+1)}{\sigma^*+1}}$	$\gamma<1:\frac{\eta+\gamma-1}{1-\gamma}$	0	$\sqrt{\eta+\gamma-1}\arctan\sqrt{\eta+\gamma-1}$
			$\gamma>1:\infty$	$\sqrt{\frac{\gamma-1}{2}}\arctan\sqrt{\gamma-1}$	
2		$\sqrt{\frac{\eta+(\gamma-1)(\sigma^*+1)}{\left(\frac{\sigma^2}{f^2}+1\right)(2\sigma^*+1)}}\arctan\sqrt{\frac{\eta+(\gamma-1)(\sigma^*+1}{\sigma^*+1}}$	$\gamma<1:\frac{\eta+\gamma-1}{1-\gamma}$	0	$\sqrt{\eta+\gamma-1}\arctan\sqrt{\eta+\gamma-1}$
			$\gamma>1:\infty$	0	
3	Fast mode without CISK mode	$\sqrt{\frac{\gamma-1}{2\left(\frac{\sigma^2}{f^2}+1\right)}}\arctan\sqrt{(\gamma-1)}$	$\gamma<1:$	no unstable solution	
			$\gamma>1:\infty$	0	$\sqrt{\frac{\gamma-1}{2}}\arctan\sqrt{\gamma-1}$
4		$\sqrt{\frac{(\gamma-1)(\sigma^*+1)}{\left(\frac{\sigma^2}{f^2}+1\right)(2\sigma^*+1)}}\arctan\sqrt{(\gamma-1)}$	$\gamma<1:$	no unstable solution	
			$\gamma>1:\infty$	0	$\sqrt{\gamma-1}\arctan\sqrt{\gamma-1}$
5		$\sqrt{\frac{(\gamma-1)(\sigma^*+1)}{2\sigma^*+1}}\arctan\sqrt{(\gamma-1)}$	$\gamma<1:$	no unstable solution	
			$\gamma>1:\infty$	$\sqrt{\frac{\gamma-1}{2}}\arctan\sqrt{\gamma-1}$	$\sqrt{\gamma-1}\arctan\sqrt{\gamma-1}$

TABLE 1. CONTINUED

Row (1)	Model (2)	Matching condition $b/R =$ (3)	Max. growth σ^* (4)	Scale b/R of max. growth b_{MIN}/R (5)	Scale b/R of zero growth b_{MAX}/R (6)
6	CISK mode without fast mode	$\sqrt{\frac{\eta-\sigma^*-1}{2\sigma^*+1}}\arctan\sqrt{\frac{\eta-\sigma^*-1}{\sigma^*+1}}$	$\gamma=0:\eta-1$	0	$\sqrt{\eta-1}\arctan\sqrt{\eta-1}$
7		$\sqrt{\frac{\eta-\sigma^*-1}{\left(\frac{\sigma^2}{f^2}+1\right)(2\sigma^*+1)}}\arctan\sqrt{\frac{\eta-\sigma^*-1}{\sigma^*+1}}$	$\gamma=0:\eta-1$	0	$\sqrt{\eta-1}\arctan\sqrt{\eta-1}$

This table sets out the characteristics and instability properties of the two-layer model described in Eqs. (1) and Fig. (2).
Column 2 lists the instability modes present.
Column 3 shows the relationship between horizontal scale b/R and non-dimensional growth rate σ^*.
Column 4 shows the maximum value of growth rate σ^*_{MAX}.
Column 5 shows the horizontal scale b_{MIN}/R at which the maximum growth-rate occurs.
Column 6 shows the horizontal scale b_{MAX}/R at which zero growth occurs.
Dynamical constraints of particular model configurations and some examples of authors using them are as follows:
Row 1 Balanced; Ekman boundary conditions; $\lambda_1 = 0$; $\lambda_2 = 1$. Charney and Eliassen (1964)
Row 2 Unbalanced; Ekman boundary conditions; $\lambda_1 = 1$; $\lambda_2 = 1$. Mak (1981)
Row 3 Unbalanced; zero lower boundary condition; $\lambda_1 = 1$; $\lambda_2 = 0$. Lilly (1960)
Row 4 Unbalanced; Ekman boundary conditions; $\lambda_1 = 1$; $\lambda_2 = 1$. Fraedrich and McBride (1994)
Row 5 Balanced; Ekman boundary conditions; $\lambda_1 = 0$; $\lambda_2 = 1$. Fraedrich and McBride (1994)
Row 6 Balanced; Ekman boundary conditions; $\lambda_1 = 0$; $\lambda_2 = 1$. Ooyama (1964), Charney (1973) and Fraedrich and McBride (1989)
Row 7 Unbalanced; Ekman boundary conditions; $\lambda_1 = 1$; $\lambda_2 = 1$. Mak (1981).
For references and notation see text.

the unbalanced models, but at finite radius $b_{\mathrm{MIN}}/R = \sqrt{\frac{\gamma-1}{2}}$ arctan $\sqrt{\gamma-1}$ for the balanced model.

The slow, or classical CISK, mode ($\eta > 1$, $\gamma = 0$) is represented by rows 6 and 7. Here the total heating is proportional to the Ekman pumping at the lower boundary. These modes have finite maximum growth-rate $\sigma^*_{\mathrm{MAX}} = \eta - 1$. It occurs, however, at vanishingly small spatial scale b/R.

Both slow and fast modes were mentioned by Charney and Eliassen (1964), Mak (1981) and others, but the fast modes have been rejected as unphysical. In Charney and Eliassen (1964) they emerged in connection with excessive humidity values associated with the particular parametrization of γ in the cumulus parametrization scheme. Bates (1973) noted the potential violation of the basic underlying assumption that the interior flow is no longer balanced at finite width, b/R, if $\sigma \gg f$. Mak (1981) also rejected these modes as unphysical, but did not elaborate in greater detail. Thus the slow modes are commonly associated with the CISK-type growth of tropical disturbances. However, their growth rates appear to be very slow and there is no natural cut-off at the short-wave end of the unstable disturbances, that is $b \to 0$ for maximum finite σ (see also Chang and Williams 1974; Pedersen and Rasmussen 1985). Furthermore, a link between the cumulus parametrization and the moisture budget needs to be established in the framework of the prescribed model structure. This leads to a new interpretation of the CISK-type instability and will be discussed in the following subsections.

(*b*) *The moisture budget*

Referring to the model geometry as depicted in Fig. 2, the total heating in a vertical column equals $\int_0^4 (Q/g)\mathrm{d}p = \int_1^3 (Q/g)\mathrm{d}p = (Q_2/g)\Delta p$. By consideration of conservation of equivalent potential temperature (or moist static energy) in a vertical column, this equals the vertical integral of $-L(\mathrm{d}q/\mathrm{d}t)$ with respect to mass, i.e.

$$Q_2 \frac{\Delta p}{g} = -L \int_0^4 \frac{\mathrm{d}q}{\mathrm{d}t} \frac{\mathrm{d}p}{g} \tag{4}$$

where L is the coefficient of latent-heat release and q is the mixing ratio of water vapour. Removing the denominator g from both sides of the equation, and expanding the substantive derivative, the total heating can be expressed as follows:

$$Q_2 \Delta p = -L \int_0^4 \left(\frac{\partial q}{\partial t} + \nabla \cdot q\mathbf{V} + \frac{\partial \omega q}{\partial p} \right) \mathrm{d}p \tag{5}$$

$$= -L \int_0^4 \left(\frac{\partial q}{\partial t} + \nabla \cdot q\mathbf{V} \right) \mathrm{d}p - L\omega_4 q_4 \tag{6}$$

(neglecting the terms $\int (\partial q/\partial t)\, \mathrm{d}p$, $\int \mathbf{V} \cdot \nabla q\, \mathrm{d}p$)

$$= -L \int_0^4 q \nabla \cdot \mathbf{V}\, \mathrm{d}p - L\omega_4 q_4, \tag{7}$$

$$= +L \int_0^4 q \frac{\partial \omega}{\partial p} - L\omega_4 q_4 \tag{8}$$

(integrating by parts)

$$= +L[\omega q]_0^4 - L \int_0^4 \omega \frac{\partial q}{\partial p} \mathrm{d}p - L\omega_4 q_4 \tag{9}$$

$$= -L \int_0^4 \omega \frac{\partial q}{\partial p} \mathrm{d}p. \tag{10}$$

(c) The cumulus parametrization of Charney and Eliassen (1964)

The above moisture budget and, in particular, Eq. (10) were originally derived for this model by CE64 (their equation (3.2)). They evaluated the integral in Eq. (10) by assuming $\partial q/\partial p$ to be constant through the depth of the troposphere and that its variations are governed by an externally specified relative humidity μ. Thus, following their parametrization, (10) becomes

$$\begin{aligned} Q_2 \Delta p &= -L\mu \left[\frac{\partial q_s}{\partial p}\right] \int_0^4 \omega \, \mathrm{d}p \\ &= -L\mu \left[\frac{\partial q_s}{\partial p}\right] \left\{\frac{\omega_2}{2}\Delta p + \frac{\omega_2 + \omega_4}{2}\Delta p\right\} \\ &= -L\mu \left[\frac{\partial q_s}{\partial p}\right] \left(\omega_2 + \frac{1}{2}\omega_4\right) \Delta p \end{aligned} \tag{11}$$

where $[\partial q_s/\partial p]$ is a mean tropical value of the vertical gradient in saturation specific humidity $q_s(T,\ p)$. Consistency between Eq. (11) and the thermodynamic equation from Eqs. (1) at level 2, $Q_2 = -(c_p pS/\mathrm{R_d})(\eta\omega_4 + \gamma\omega_2)$ requires that

$$\frac{c_p p}{\mathrm{R_d}} S\gamma = L\mu \left[\frac{\partial q_s}{\partial p}\right] \qquad \eta = \frac{\gamma}{2}. \tag{12}$$

Substituting the values of $(\gamma,\ \eta)$ from (12) into the width–growth relation (2) yields the curves plotted by CE64 and reproduced in Fig. 1(a) (where we note that the width–growth relation of CE64 differs slightly from Eq. (2) due to their use of cylindrical geometry). Using this convective parametrization, the growth-rate curve depends critically on the external parameter μ (relative humidity) and, in particular, undergoes a rapid transition from the slow, CISK, mode to the fast mode in the parameter range $\mu = (0.8,\ 1.0)$.

(d) A cumulus parametrization based on underlying sea surface temperature

Firstly we consider the moisture budget. If we consider moisture to be carried at the middle level 2 and the lower boundary 4, the integration in Eq. (10) can be carried out as follows

$$Q_2 \Delta p = -L \left\{ \underbrace{\frac{\omega_2}{2} q_2}_{\text{upper layer}} + \underbrace{\frac{\omega_4 + \omega_2}{2}(q_4 - q_2)}_{\text{lower layer}} \right\} \tag{13}$$

$$= -\frac{L}{2}\{\omega_2 q_4 + \omega_4 (q_4 - q_2)\}. \tag{14}$$

Comparing Eq. (14) with the thermodynamic equation $Q_2 = -(c_p pS/\mathrm{R_d})(\eta\omega_4 + \gamma\omega_2)$ gives the following values for γ and η

$$\gamma = \frac{L}{2}\frac{\mathrm{R_d}}{c_p}\frac{1}{pS\Delta p} q_4 \qquad \eta = \gamma\left(1 - \frac{q_2}{q_4}\right). \tag{15}$$

Secondly we consider a simple boundary layer. In Eq. (15) q_4 is the value of moisture at the lower boundary of the model. Consistent with the formulation of CE64, this is the top of the Ekman boundary-layer. If we assume constant potential temperature within the boundary layer (i.e. a well-mixed layer) and we also assume a relative humidity of 85% at the top of the mixed layer, then

$$\begin{aligned} q_4 &= 0.85 q_s(T_4,\ p_4) \\ &\approx 0.85 q_s\left(T^*\left(\frac{1000}{p_4}\right)^{-\mathrm{R_d}/c_p},\ p_4\right) \end{aligned} \tag{16}$$

where the functional $q_s(T,\ p)$ is the saturation mixing ratio.

Setting the lower boundary of the model at 900 hPa, and substituting Eq. (16) into Eq. (15), yields the following relationship between the heating parameter γ, static stability S, and the underlying SST T^*

$$\gamma = \frac{L}{2}\frac{\mathrm{R_d}}{c_p}\frac{1}{pS(\Delta p)} \times 0.85 q_s\left(T^*\left(\frac{1000}{p_4}\right)^{-\mathrm{R_d}/c_p},\ p_4\right). \tag{17}$$

To solve Eq. (2) all that remains is the specification of the second heating parameter η. As will be shown later, the behaviour of the solutions is dominated by γ, so for the purposes of this study, we shall simply specify $\eta = \gamma/2$ (which is the value used by CE64 and means that in Eq. (15) $q_2/q_4 \simeq \frac{1}{2}$).

3. SSTs AND GROWTH RATES OF TROPICAL DISTURBANCES

Substituting Eq. (17) into Eq. (2) and using $\eta = \gamma/2$ yields a relationship between growth rate σ and the horizontal scale b for a given value of SST T^*. This relationship is plotted in Fig. 1(b) for a range of values of T^*. The values used for the other constants are as follows: $S = 2 \times 10^{-2}\ \mathrm{m^2 sec^{-2} hPa^{-2}}$, $\Delta p = 450$ hPa, $K = 50$ hPa, $f = 0.377 \times 10^{-4}\mathrm{sec}^{-1}$ (at latitude 15°).

The growth-rate curves fall into two families according to whether or not γ exceeds one (i.e. T^* exceeds 25.5 °C). For lower values of SST, the maximum growth-rate occurs at the smallest scale; this solution corresponds to a dominance of the classical CISK mode of CE64 (Ooyama 1964, 1969; Fraedrich and McBride 1989). For SSTs exceeding 25.5 °C, infinitely large growth-rates are observed at finite horizontal scales which agree roughly with those of the cloud cluster or tropical cyclone in nature.

An alternative representation of the solutions is given in Fig. 3 which shows the path of the scale of zero growth (i.e. $\sigma^* = 0$) and the path of the scale of infinite growth ($\sigma^* = \infty$) as a function of SST. The shaded area represents the region in (b, T^*) space for which there are unstable solutions. The large (infinite) growth-rates occur when the lower curve departs from the lower axis; and this occurs at a transition temperature of 25.5 °C. It is noteworthy that this transition also marks the beginning of growth at large scales, i.e. the meso-α and synoptic scales of convection over tropical oceans observed in nature. The upper curve is the plot of b_{MIN}/R while the lower curve is that of b_{MAX}/R, both from row 1 of Table 1. Thus the scale of maximum growth (i.e. the outer curve) depends only on the underlying SST (through the parameter γ) and not on the mid-level humidity (through η).

At this stage it should be noted that the model used is that from row 1 of Table 1, and is based on the *balanced* version of the equations ($\lambda_1 = 0$). The balance condition is only

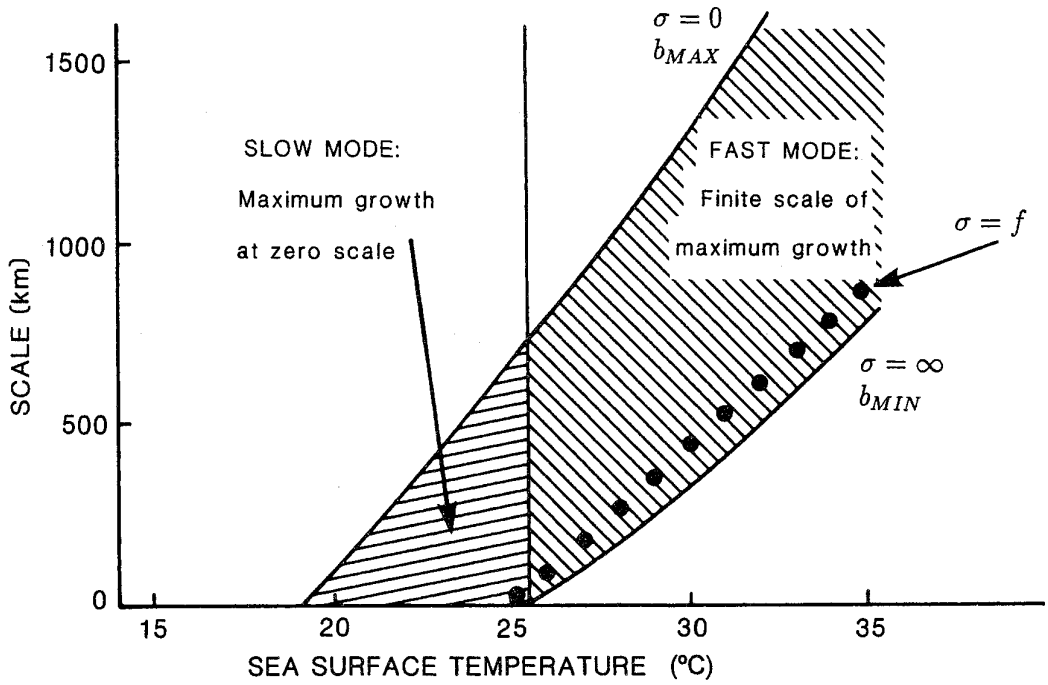

Figure 3. Domain of instability: the maximum and minimum half-width, $b_{\mathrm{MAX}} = b(SST,\ \sigma = 0)$, and $b_{\mathrm{MIN}} = b(SST,\ \sigma = \infty)$ of unstable balanced perturbations as a function of the underlying sea surface temperature. The structure change between fast and slow modes occurs at 25.5 °C where the minimum width b_{MIN} first exceeds zero and the maximum growth-rate first becomes infinite.

valid (and so therefore are the solutions) when σ is smaller than the Coriolis parameter f. The horizontal line $\sigma = f$ is plotted in Fig. 1(b), where the intercept with this line at high SSTs (28 to 30 °C) occurs at scales between 100 and 1000 km. It is our basic hypothesis that the slow (balanced) flow will occur at these scales and growth rates, which mark the upper limit of validity of the balanced assumption. Following this philosophy the lower line in Fig. 3 may be replaced by the line of heavy dots, which is the path of the intercept of the solution with $\sigma = f$.

4. Discussion

In this paper we have shown that through a simple re-formulation of the cumulus parametrization scheme, the classical 2-layer model of Charney and Eliassen (1964) can provide a theory for the rapidly changing response of oceanic tropical convection to variations in the underlying SST. The immediate question that arises is whether or not this is the dominant physical mechanism responsible for this phenomenon in nature.

In this context there have been several recent criticisms of CISK-type instabilities. Emanuel (1989) states that the CISK models make an incorrect assumption of the existence of a reservoir of Convective Available Potential Energy (CAPE) to drive the large-scale motions. Strictly this is not correct as CAPE does not appear explicitly in the basic Eqs. (1) used by CE64. The criticism does, however, highlight the major weakness of this class of models in that the major component of the physics is contained in the heating equation $Q_2 = -(c_p p/\mathrm{R_d})S(\eta\omega_4 + \gamma\omega_2)$. To give values to the coefficients γ, η requires interpretation of the model in terms of a moisture budget. As shown in the present paper, the interpretation of the results can vary significantly depending on how this moisture budget is constructed: e.g. the parametrization of CE64 versus the SST-based parametrization. Thus, until they are extended to include an explicit moisture budget, the CISK-type models

embody an incomplete theory. The present paper explicitly sets the local time-derivative of moisture to zero in Eq. (7). This can be extended, following the philosophy of Kuo (1974), to an assumption that the vertically integrated moistening of the column is a small parameter b_{KUO} times the vertically integrated three-dimensional convergence of moisture

$$\int_0^4 \frac{\partial q}{\partial t} \mathrm{d}p = -b_{\mathrm{KUO}} \int_0^4 \left(\nabla \cdot q\mathbf{V} + \frac{\partial \omega q}{\partial p} \right) \mathrm{d}p. \tag{18}$$

Substituting into Eq. (5) and carrying the parameter through in the subsequent algebra gives the result

$$\gamma = (1 - b_{\mathrm{KUO}}) \frac{L}{2} \frac{\mathrm{R_d}}{c_p} \frac{1}{pS\Delta p} q_4 \qquad \eta = \gamma \left(1 - \frac{q_2}{q_4} \right) \tag{19}$$

so that the analysis in the present paper remains essentially unchanged. As discussed, however, by McBride *et al.* (1989) the Kuo assumption Eq. (18) is not supported by observation; so the lack of an explicit moisture equation still remains as the major weakness of the current model.

Montgomery and Farrell (1993) criticized CISK models on the grounds that the Ekman lower boundary condition ($\omega_4 = \lambda_2 K(\partial u_3/\partial y)$ is valid only 'after an incipient vortex has attained sufficient strength and organization so that the cloud-organizing mesoscales are correlated with the balanced flow'. The results of the present paper show that the scales of preferred growth for the fast mode are of the order of several hundred kilometres (for the half-width of the disturbance). The question is whether tropical motions on that scale can be considered quasi-geostrophic, and, in particular, whether or not the Ekman boundary condition is valid on those scales. The validity of CISK-type models depends totally on this question, which deserves further investigation. In this context we note the study of Stout and Young (1983) who carried out a balance-of-forces analysis for the large-scale monsoonal flow during the 1979 International Monsoon Experiment (MONEX). According to their results, the low-level flow is quasi-geostrophic beyond about 5 degrees of latitude from the equator (see their Fig. 9).

Besides the balance assumption (and its accompanying Ekman lower boundary condition), the other basic assumption of our analysis is that the vertically integrated heating is dominated by the underlying SST (as in our formulation) rather than by the relative humidity (as in the CE64 formulation). This assumption can be considered to be a form of 'quasi-equilibrium hypothesis' whereby surface evaporation acts to bring the low-level air into equilibrium with the underlying sea. Thus the model sensitivity is dominated by an external parameter (the SST) as distinct from an essentially internal parameter (the relative humidity) as was the case in the CE64 formulation.

A last caveat that should be noted is that the constants used to produce Figs. 1(b) and 3 gave the cut-off temperature at approximately 25.5 °C. There is some sensitivity of the solutions to the choice of constants, particularly the static stability S. Equation (17) was interpreted above as a relationship between γ and T^*. The transition temperature marking the onset of the fast mode occurs at $\gamma = 1$. Substituting for γ, Eq. (17) then becomes an expression for the threshold SST as a function of static stability S.

In this context, we note that Rasmussen (1979) has hypothesized that arctic polar lows may be manifestations of CISK. Static stability S has a slightly higher value at the poles than in the tropics, but the depth of troposphere Δp through which the development takes place is approximately half that in the tropics; thus, through Eq. (17), the transition, $\gamma = 1$, can occur at a lower temperature, so that the explosive growth of polar lows may also be associated with the transition to the fast mode. There is also evidence that explosively

growing lows off the eastern coastlines of Australia (Holland *et al.* 1987; McInnes *et al.* 1992) and of the USA (Sanders and Gyakum 1980; Gyakum and Barker 1988) may be warm-cored systems embedded within a larger-scale baroclinic low. In such cases, it is also possible that the embedded explosively growing system may be a manifestation of the transition to the fast mode. For the United States east-coast lows there is some supporting evidence that the static stability S is observed to decrease (thereby increasing γ through Eq. (17)) before, or in the early stages of, development (Gyakum and Barker 1988).

It is also instructive to interpret the change in behaviour at a threshold SST in terms of the 'effective static stability' concept, introduced by Fraedrich and McBride (1995). The basic reason for the existence of a threshold value of SST is that the fast-mode component of heating leads to the appearance of the coefficient $S(1-\gamma)$ modifying the vertical motion term ω_2 in the thermodynamic equation of Eqs. (1). Thus, as the underlying SST increases, the available moisture increases; this increases the coefficient γ until a threshold SST is reached whereby γ exceeds the value one. At this point the 'effective static stability' $S(1-\gamma)$ becomes negative, the large-scale flow becomes effectively statically unstable and a large-scale convective overturning takes place. The properties and physical meaning of large-scale balanced flows with negative effective static stability and an Ekman lower boundary have been explored in a recent paper by the present authors (Fraedrich and McBride 1995).

Acknowledgements

This research developed from an extended visit by the first author to the Freie Universität Berlin during 1989. The Humboldt Foundation, the Freie Universität and the Bureau of Meteorology Research Centre are all thanked for sponsoring that visit. After the preparation of this paper, we learned that some of these ideas were anticipated in a University of Hamburg Tropical Meteorology Seminar note by Thomas Frisius.

References

Bates, J. R. 1973 A generalization of the CISK theory. *J. Atmos. Sci.*, **30,** 1509–1519

Chang, C. P. and Williams, R. T. 1974 On the short-wave cut-off of CISK. *J. Atmos. Sci.*, **31,** 830–833

Charney, J. G. and Eliassen, A. 1964 On the growth of the hurricane depression. *J. Atmos. Sci.*, **21,** 68–75

Charney, J. G. 1973 Planetary fluid dynamics. Chapt. 13: Tropical cyclogenesis and the formation of the intertropical convergence zone. *Dynamical Meteorology*, Ed. P. Morel, Reidel Publ., Dordrecht, 331–344

Emanuel, K. 1989 The finite-amplitude nature of tropical cyclogenesis. *J. Atmos. Sci.*, **46,** 3431–3456

Evans, J. L. 1993 Sensitivity of tropical cyclone intensity to sea surface temperature. *J. Climate*, **6,** 1133–1140

Fraedrich, K. and McBride, J. L. 1989 The physical mechanism of CISK and the free-ride balance. *J. Atmos. Sci.*, **46,** 2642–2648

1995 Large scale convective instability revisited. *J. Atmos. Sci.*, **52,** in press

Gray, W. M. 1968 Global view of the origin of tropical disturbances and storms. *Mon. Weather Rev.*, **96,** 669–700

Gyakum, J. R. and Barker, E. S. 1988 A case study of explosive subsynoptic-scale cyclogenesis. *Mon. Weather Rev.*, **116,** 2225–2253

Holland, G. J., Lynch, A. H. and Leslie, L. M. 1987 Australian east coast cyclones. Part I: Synoptic overview and case study. *Mon. Weather Rev.*, **115,** 3024–3036

Kuo, H. L. 1974 Further studies of the parameterization of the influence of convection on large-scale flow. *J. Atmos. Sci.*, **31,** 1232–1240

Lau, K. M. and Chan, P. H. 1988 Intraseasonal and interannual variations of tropical convection: A possible link between the 40-day mode and ENSO. *J. Atmos. Sci.*, **45,** 950–972

Lilly, D. K. 1960 On the theory of disturbances in a conditionally unstable atmosphere. *Mon. Weather Rev.*, **88,** 1–17

Mak, M. 1981 An inquiry on the nature of CISK, Part I. *Tellus*, **33,** 531–537

McBride, J. L., Gunn, B. W., Holland, G. J., Keenan, T. D. and Davidson, N. E. 1989 Time series of total heating and moistening over the Gulf of Carpentaria radiosonde array during AMEX. *Mon. Weather Rev.*, **117,** 2701–2713

McInnes, K. L., Leslie, L. M. and McBride, J. L. 1992 Simulations of Australian east coast cut-off lows: Sensitivity to sea surface temperature. *Int. J. Climatol.*, **8,** 783–795

Merrill, R. T. 1988 Environmental influences on hurricane intensification. *J. Atmos. Sci.*, **45,** 1132–1151

Montgomery, M. T. and Farrell, B. F. 1993 Tropical cyclone formation. *J. Atmos. Sci.*, **50,** 285–310

Ooyama, K. 1964 A dynamical model for the study of tropical cyclone development. *Geophys. Int.*, **4,** 187–198

1969 Numerical simulation of the life cycle of tropical cyclones. *J. Atmos. Sci.*, **26,** 3–40

Palmén, E. 1948 On the formation and structure of tropical hurricanes. *Geophysica*, **3,** 26–38

Pedersen, T. S. 1991 A comparison of the free ride and CISK assumptions. *J. Atmos. Sci.*, **48,** 1813–1821

Pedersen, T. S. and Rasmussen, E. 1985 On the cut-off problem in linear CISK-models. *Tellus*, **37A,** 394–402

Rasmussen, E. 1979 The polar low as an extratropical CISK disturbance. *Q. J. R. Meteorol. Soc.*, **105,** 531–549

Sanders, F. and Gyakum, J. R. 1980 Synoptic-dynamic climatology of "the bomb". *Mon. Weather Rev.*, **108,** 1589–1606

Stout, J. E. and Young, J. A. 1983 Low-level monsoon dynamics derived from satellite winds. *Mon. Weather Rev.*, **111,** 774–798

Webster, P. J. and Lukas, R. 1992 TOGA COARE: The coupled ocean-atmosphere response experiment. *Bull. Am. Meteorol. Soc.*, **73,** 1377–1416

Wiin-Nielsen, A. 1993 Studies of CISK. *Atmósphera*, **6,** 51–77